BIOCHEMISTRY
including biophysical chemistry & molecular biology

ARTICLE

pubs.acs.org/biochemistry

Presence of Divalent Cation Is Not Mandatory for the Formation of Intramolecular Purine-Motif Triplex Containing Human *c-jun* Protooncogene Target

Shikha Kaushik,[†] Mahima Kaushik,[†] Fedor Svinarchuk,[‡] Claude Malvy,[‡] Serge Fermandjian,[‡] and Shrikant Kukreti*[,†]

[†]Nucleic Acids Research Laboratory, Department of Chemistry, University of Delhi (North Campus), Delhi 110007, India

[‡]Vectorologie et Transfert de Genes, UMR 8121 CNRS, and Departement de Biologie et Pharmacologie Structurales, UMR 8113 CNRS LBPA (ENS Cachan), Institut Gustave Roussy, 94805 Villejuif Cedex, France

ABSTRACT: Modulation of endogenous gene function, through sequence-specific recognition of double helical DNA via oligonucleotide-directed triplex formation, is a promising approach. Compared to the formation of pyrimidine motif triplexes, which require relatively low pH, purine motif appears to be the most gifted for their stability under physiological conditions. Our previous work has demonstrated formation of magnesium-ion dependent highly stable intermolecular triplexes using a purine third strand of varied lengths, at the purine•pyrimidine (Pu•Py) targets of SIV/HIV-2 (*vpx*) genes (Svinarchuk, F., Monnot, M., Merle, A., Malvy, C., and Fermandjian, S. (1995) *Nucleic Acids Res. 23*, 3831−3836). Herein, we show that a designed intramolecular version of the 11-bp core sequence of the said targets, which also constitutes an integral, short, and symmetrical segment $(G_2AG_5AG_2)$•$(C_2TC_5TC_2)$ of human *c-jun* protooncogene forms a stable triplex, even in the absence of magnesium. The sequence d-$C_2TC_5TC_2T_5G_2AG_5AG_2T_5G_2AG_5AG_2$ (I-Pu) folds back twice onto itself to form an intramolecular triple helix via a double hairpin formation. The design ensures that the orientation of the intact third strand is antiparallel with respect to the oligopurine strand of the duplex. The triple helix formation has been revealed by nondenaturating gel assays, UV-thermal denaturation, and circular dichroism (CD) spectroscopy. The monophasic melting curve, recorded in the presence of sodium, represented the dissociation of intramolecular triplex to single strand in one step; however, the addition of magnesium bestowed thermal stability to the triplex. Formation of intramolecular triple helix at neutral pH in sodium, with or without magnesium cations, was also confirmed by gel electrophoresis. The triplex, mediated by sodium alone, destabilizes in the presence of 5′-$C_2TC_5TC_2$-3′, an oligonucleotide complementary to the 3′-oligopurine segments of I-Pu, whereas in the presence of magnesium the triplex remained impervious. CD spectra showed the signatures of triplex structure with A-like DNA conformation. We suggest that the possible formation of pH and magnesium-independent purine-motif triplexes at genomic Pu•Py sequences may be pertinent to gene regulation.

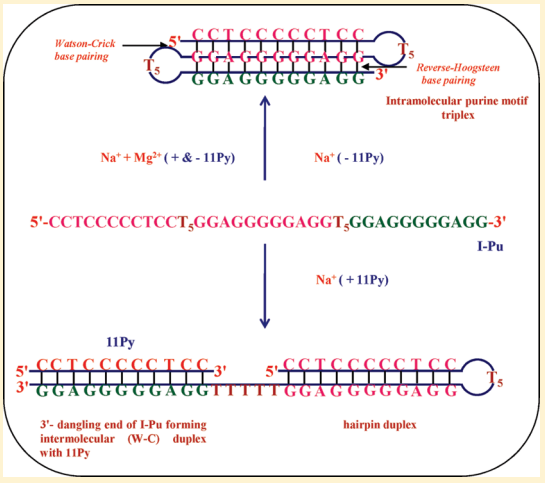

Though the existence of triple-stranded structures formed by synthetic homopurine−homopyrimidine sequences was reported several decades ago,[1] the suggestions that such structures could have biological and therapeutic roles came in the late 80s (reviewed in refs 2 and 3). The sequence-specific recognition of a double-stranded DNA (ds DNA) by a short oligonucleotide takes place through its binding into the major groove, resulting in a local triple helix. This recognition process is based on specific hydrogen bonding between nucleobases of the third strand and the purine bases of the Watson−Crick duplex.[4]

Triplexes are classified into at least three main categories that differ in the sequence composition of the third strand (triplex forming oligonucleotide, TFO) and its orientation with respect to the polypurine Watson−Crick target strand. The first class, called the pyrimidine motif, includes binding of the polypyrimidine third strand (C T, ODNs) to the duplex, in a parallel orientation, by Hoogsteen hydrogen bond forming T•A•T and $C•G_*C^+$ base triplets. For stability of such structures, cytosine must be protonated making these triplexes pH dependent.[5−7] However, the incorporation of 5-methylcytosine instead of cytosine in such TFOs increases the stability of these triplexes at the physiological pH.[8] In the second class, known as the purine motif, the polypurine third strand (G A, ODNs) binds in an antiparallel orientation to the polypurine strand of the duplex by

Received: August 6, 2010
Revised: March 7, 2011
Published: March 07, 2011

reverse Hoogsteen hydrogen bonds, forming T•A*A and C•G*G triplets. These TFOs bind to the duplex at and near neutral pH; however, their formation depends on multivalent cations such as Mg^{2+} or spermine.[9,10] An estimated value of these cations inside the cell indicates that their intracellular concentration supports the triplex formation. In the third catagory, the third strand containing G T can form triplexes with either Hoogsteen/reverse—Hoogsteen hydrogen bonding interactions and have parallel or antiparallel orientation with respect to the target polypurine strand, respectively. It has been shown that the preferred strand orientation depends on the sequence of the oligonucleotide. The formation of both (G, A) and (G, T) motif triple helices such as the purine motif is pH independent and requires the presence of divalent cations in the millimolar range.[11,12] The structure and stability of triple-helical DNA have been the subject of several excellent reviews.[2,13]

Interestingly, triple-stranded structures have not only been confined to synthetic oligonucleotides, but they have also been shown to occur intramolecularly at purine•pyrimidine tracts in supercoiled plasmids.[14] The studies of Kohwi and Kohwi-Shigematsu deserve particular attention, where they applied a fine structure mapping technique to supercoiled plasmid DNA to study the unusual DNA structure adopted by the poly(dG)•poly(dC) sequence under torsional stress at pH 5 and various ionic conditions.[15] The results led to the suggestion that the poly(dG)•poly(dC) stretch is folded into halves from the center of the sequence to form either a triplex consisting of poly(dC)•poly(dG)*poly(dG) in the presence of magnesium with the two dG strands running antiparallel to each other or a triplex consisting of poly(dC)•poly(dG)*poly(dC^+) in the absence of magnesium with one of the dC strands protonated and running parallel to the dG strand. These results clearly demonstrated that pyr•pur*pur and pyr•pur*pyr triplexes can exist in the same system under different solution conditions. This biomolecular triplex formed from partially unwound duplex DNA was shown to form in vivo, proposed to be involved in transcriptional regulation and replication.[16−18]

Although TFOs are promising tools for gene therapy,[19−21] new strategies to increase the stability and binding affinity of the ODNs involved in triplex formation are being investigated.[22,23] Targeting DNA by triplex forming oligonucleotides offers a wide range of potential applications in medicine and biotechnology including the site-specific inhibition of transcription[24,25] or the development of sequence-specific artificial nucleases, for example, for chromosome mapping.[26] In the biomedical field, however, antiparallel triplexes using duplex ODNs are more promising than parallel structures as the formation of antiparallel triplex is pH independent.[27−29]

Single-stranded oligonucleotides of appropriate sequence can provide a good model system for studying triplexes in an intramolecular topology, as they constitute the triple strand part of H-DNA.[3] In the present study, we investigated intramolecular purine motif triplex formation using native polyacrylamide gel electrophoresis, UV-thermal denaturation, and circular dichroism (CD) spectroscopy. The target for the studied oligonucleotide, 5′-GGAGGGGGAGG-3′, is found in a highly conserved 20-bp long purine/pyrimidine sequence of human *c-jun* protooncogene and is also present in many mammalian genes, for instance, in the promoter sequence of bovine cytokeratin,[30] human major histocompatibility class III HLA factor B,[31] *vpx* gene of SIV/HIV-2, *c-pim* protooncogene, etc. We show here that the formation of an intramolecular triplex in purine motif does not require the divalent cation magnesium, known to be mandatory for its intermolecular version antiparallel triplexes.[32,33] However, the presence of magnesium stabilizes the triplex. The designed sequence d-$C_2TC_5TC_2T_5G_2AG_5AG_2T_5G_2AG_5AG_2$ (I-Pu) containing the said target forms an intramolecular triple helix with 11 base triplets and 2 T_5 loops by folding back twice on themselves under appropriate solution conditions. The use of such a molecule had been adopted because it avoids strand stoichiometry problems, and because of its increased stability due to the intramolecular nature of the structure, it disfavors competing secondary structures such as homoduplexes, G-Quartets, and C-Quartets at or near physiological pH. Such intramolecular folded constructs are particularly valuable in thermodynamics[34] and NMR structural studies of triple helices.[35,36]

MATERIALS AND METHODS

The oligonucleotides synthesized in micromolar scale by Bio. Basic Inc., Canada, were received in the lyophilized powder form. They were stored at −20 °C and were used without further purification. The concentration of the oligonucleotides was determined spectrophotometrically by using the extinction coefficient (ε) calculated by the nearest neighbor method[37] and by measuring the absorbance at 260 nm. The ε values used for the 43-mer oligonucleotide sequence d-CCTCCCCCTCCTTTTTGGAGGGGGAGGTTTTTGGAGGGGGAGG (I-Pu), 11-mer d-GGAGGGGGAGG (11Pu), and 11-mer d-CCTCCCCCTCC (11Py) were 397 300, 118 700, and 81 200 M^{-1} cm^{-1}, respectively. Oligonucleotides d-CTTGAGCTCAAG (PAL12, ε = 113 700 M^{-1} cm^{-1}), d-GACTGACTTAAGCGCATAGCTAGCTCGATAGCTGA (M35, ε = 342 600 M^{-1} cm^{-1}), and d-CTTGAGCTTGAG CTCAAGCTCAAG (PAL24, ε = 226 100 M^{-1} cm^{-1}) were used as control size markers in gel assays.

The stock solutions of the oligomers were prepared by dissolving directly the lyophilized powder in Milli-Q water. All other chemicals were of analytical grade. The buffer solution consisted of 20 mM sodium cacodylate (pH 7.0), 0.1 mM EDTA and were adjusted to desired ionic strength with sodium chloride or magnesium chloride. The oligonucleotide samples were prepared by taking their appropriate range of strand concentrations.

UV-Thermal Denaturation. UV-thermal denaturation experiments (Tm) were performed on a UV-1650PC Shimadzu UV−vis spectrophotometer (equipped with a peltier thermoprogrammer TMSPC-8(E)-200) and interfaced with a Pentium IV computer for data collection and analysis. The stoppered quartz cuvettes of 1.0 and 0.1 cm optical path length with 110 μL and 35 μL volumes respectively were used for measurements. The temperature dependence on the absorption value of the DNA was monitored at 260 nm. The temperature of the cell holder was increased from 20 to 105 °C at a rate of 0.5 °C/min. The melting curves were normalized at lower temperature values. The thermal melting temperature (Tm) was determined from the peak of the computer generated first derivative of the absorbance versus temperature profile. The accuracy of the reported Tm values is ±1 °C.

Non-Denaturating Gel Electrophoresis. For performing non-denaturating gel experiments, oligonucleotide samples were prepared in 20 mM sodium cacodylate buffer (pH 7.0) at desired concentrations (15 μM). The final volume of the sample in the buffer was 20 μL. Importantly, prior to performing gel assays in non-denaturating conditions, the purity of the commercially

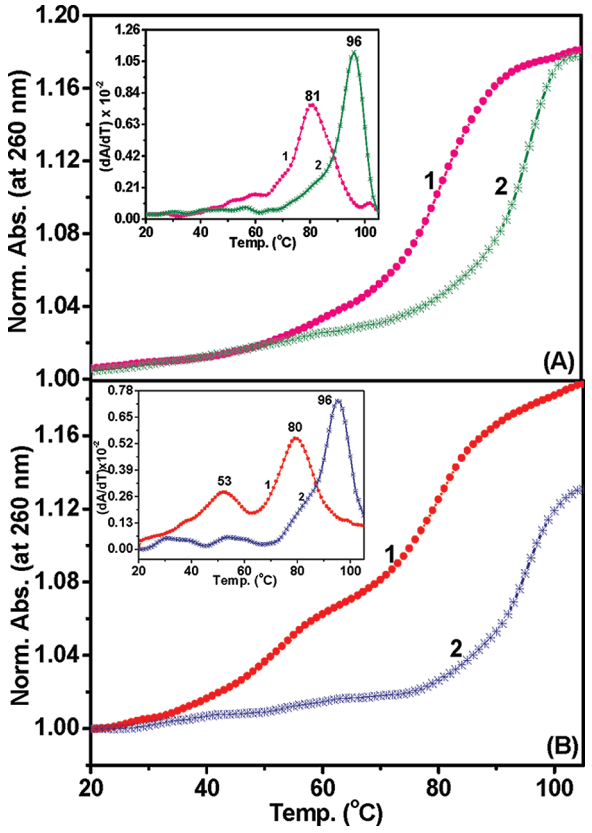

Figure 1. (A) Thermal denaturation profiles of I-Pu (d-CCT-CCCCCTCCT$_5$GGAGGGGGAGGT$_5$GGAGGGGGAGG) in 20 mM sodium cacodylate buffer (pH 7.0) and 0.1 mM EDTA containing 100 mM Na^+ (1) and 100 mM Na^+ + 10 mM Mg^{2+} (2). (B) Thermal denaturation profiles of I-Pu + 11Py (d-CCTCCCCCTCC) in 20 mM sodium cacodylate buffer (pH 7.0) and 0.1 mM EDTA containing 100 mM Na^+ (1) and 100 mM Na^+ + 10 mM Mg^{2+} (2) [inset shows the first derivative of the plot].

made oligomers was checked by running them on 20% PAGE using 8 M urea. All oligonucleotide sequences migrated as single bands, according to their sizes. For non-denaturating gel assays, the samples (20 μL) were heat treated at 95 °C for 5 min and slowly cooled to room temperature over about ~10 h. Samples were incubated at 4 °C overnight before loading onto 20% polyacrylamide gel pre-equilibrated for 1 h. The loading gel contained 20 mM sodium cacodylate (pH 7.0) with 0.1 mM EDTA containing the desired ionic strength. The running buffer was 1× TBE with 0.1 mM EDTA. The salt concentration of the solution was adjusted to the desired concentration by adding various salts. For simplicity, sodium chloride and magnesium chloride are designated as Na^+ and Mg^{2+} at appropriate places in the text. Tracking dye consisted of Orange-G with glycerol. The gels were run approximately at 8 °C at a constant voltage of 45 V as well as at room temperature (24 °C) at 40 V. After electrophoresis, the gels were stained with Stains-All (Sigma) and finally visualized under trans-white light and photographed by AlphaImager 2200 (Alpha Infotech Corp.).

Circular Dichroism Spectroscopy. For secondary structure determination, CD spectra were recorded on JASCO-715 spectropolarimeter interfaced with an IBM PC compatible computer, calibrated with D-Camphor Sulfonic acid. Four scans of the spectrum were collected over the wavelength range 200−320 nm at a scanning rate of 100 nm/min. The average of multiple scans was used for analysis. The scan of buffer alone recorded at room temperature was subtracted from the average scans for each DNA strand. Samples were recorded in a 1 cm path length quartz cuvette of 1 mL volume capacity. Data were collected in units of millidegrees versus wavelength.

RESULTS AND DISCUSSION

UV-Thermal Denaturation Studies. A thermal denaturation experiment determines the stability of oligonucleotide secondary structures. Figure 1A displays the absorbance versus temperature profile of the 43-nt I-Pu sequence [$C_2TC_5TC_2T_5G_2AG_5AG_2T_5$-$G_2AG_5AG_2$] (2 μM oligomer concentration) in 20 mM sodium cacodylate buffer (pH 7.0) containing 0.1 mM EDTA in the presence of 100 mM Na^+ (curve 1) and 100 mM Na^+ + 10 mM Mg^{2+} (curve 2). The melting curve of I-Pu was found to be monophasic in both conditions, indicating the melting of single structural species in the solution. On the basis of reports[9,29] that the presence of divalent cations is necessary for purine motif triplexes, the monophasic profile obtained in the presence of Na^+ + Mg^{2+} (Figure 1A, curve 2) can be assumed to be the single step melting of intramolecular triplex into the unstructured single strand. The triplex is assumed to be formed via the formation of a double hairpin having two T_5 loops. The melting temperatures were found to be 81 and 96 °C in Na^+ and Na^+ + Mg^{2+}, respectively. Monophasic melting transitions, reflecting the dissociation of intermolecular purine motif triplexes to single strands in one step, have also been reported by us [32,33] on SIV/HIV-2 vpx targets and others, on the sequence [$C_3T_4C_3$]•2-[d($G_3A_4G_3$)] in the presence of Mg^{2+}.[38] However, in the case of I-Pu here, melting of the mere Watson−Crick base paired duplex region (hairpin with unpaired 3′-dangling end) resulting in monophasic thermal transition, cannot be ruled out at this point.

To verify this, an additional experiment was carried out, where the formation of an intramolecular triplex structure adopted by I-Pu was monitored with and without magnesium, in the presence of a complementary oligonucleotide. Accordingly, 11-mer pyrimidine strand 5′-$C_2TC_5TC_2$-3′ (11Py), complementary to the 3′-end 11-mer segment of I-Pu, was added to I-Pu in an equimolar ratio in the presence of 100 mM Na^+without Mg^{2+} (Figure 1B, curve 1). Thermal denaturation manifested in an apparently broad and biphasic melting profile, indicating the existence of two species in the solution. Since the lower and higher temperature transitions of biphasic curve are sufficiently separated, it was easy to deduce the Tm values for the two structural species. The lower temperature transition displayed a Tm value of 53 °C, whereas for the higher temperature transition the Tm was found to be 80 °C. Thus, it clearly shows that in the presence of Na^+, 11Py forms an intermolecular 11-bp duplex, through Watson−Crick hydrogen bonding with the 3′-purine stretch of I-Pu. Following the notion that intermolecular duplex species have a lower thermal stability than their intramolecular (hairpin) counterparts,[39] it can be well assumed that the lower temperature transition (Tm 53 °C) corresponds to the melting of intermolecular duplex, whereas the higher temperature transition (Tm 80 °C) of the biphasic curve presumably corresponds to the melting of intramolecular hairpin into single-strand.

Interestingly, when 11Py is added to I-Pu in the presence of 100 mM Na^+ + 10 mM Mg^{2+} (Figure 1B, curve 2), melting transition with a Tm value of 96 °C was found to be monophasic. It indicates the melting of only one species in solution. The same

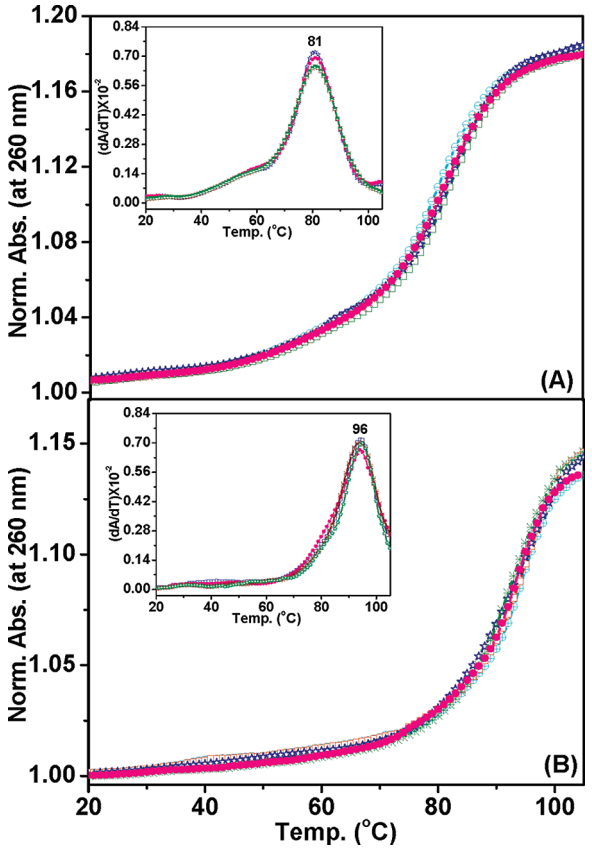

Figure 2. Thermal denaturation profiles of I-Pu in 20 mM sodium cacodylate buffer (pH 7.0) and 0.1 mM EDTA at 0.5 μM (cyan —○—), 5.0 μM (pink —●—), 15.0 μM (blue —☆—), 25.0 μM (red —□—), and 35.0 μM (green —*—) oligomer strand concentration containing 100 mM Na^+ (A) and 100 mM Na^+ + 10 mM Mg^{2+} (B) [inset shows the first derivative of the plot].

can be assumed to be the dissociation of intramolecular triplex into single strand, that is, three strands of triplex, associated through Watson−Crick and reverse−Hoogteen hydrogen bonding, opening up simultaneously.

Considering the above observations, it can be explained that the 11-mer 3′-terminal purine segment of I-Pu, when engaged in triplex formation in the presence of Na^+ + Mg^{2+} ions, is not available for Watson−Crick pairing with the added 11Py sequence and hence results in one step melting of intramolecular triplex I-Pu (Figure 1B, curve 2). On the contrary, with no Mg^{2+} in the solution, the addition of 11Py to I-Pu results in duplex formation with the 3′-purine end of I-Pu. It is clear that the presence of divalent cation Mg^{2+} not only facilitated the triplex formation but also stabilized the sodium triplex by 15 °C (Figure 1B, curve 1, 2).

Again, to confirm our interpretation of the lower temperature transition of Figure 1B (curve 1), a separate UV-melting experiment was performed on the equimolar mixture of 11Py and 11Pu [5′-$G_2AG_5AG_2$-3′] (separately synthesized 3′-purine 11-mer stretch of I-Pu), under the identical solution conditions used in Figure 1B (curve 1). Thermal denaturation resulted in a characteristic monophasic sigmoidal curve with a Tm value of 53 °C (data not shown), which is equal to the Tm of the lower temperature transition of Figure 1B (curve 1). Hence, it can easily be attributed to the melting of the Watson−Crick

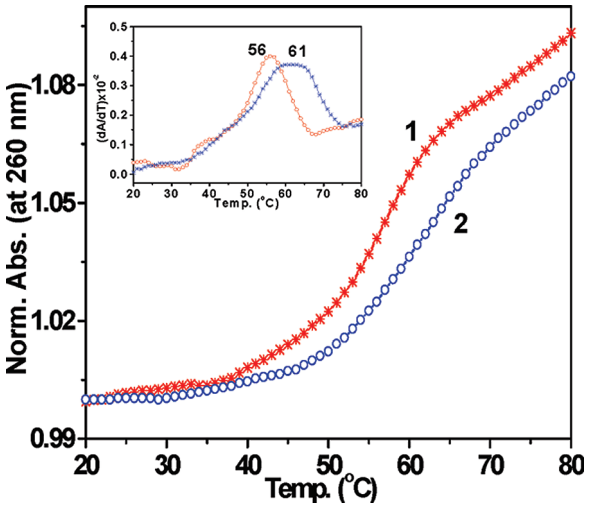

Figure 3. Thermal denaturation profiles of 11Pu + 11Py (d-GGAGGGGGAGG) + (d-CCTCCCCCTCC) in 20 mM sodium cacodylate buffer (pH 7.0) and 0.1 mM EDTA containing 100 mM Na^+ + 10 mM Mg^{2+} at a 1:1 (**1**) and 2:1 molar ratio (**2**).

hydrogen bonded intermolecular duplex formed by the pyrimidine sequence, 11Py and 3′-purine dangling end of the I-Pu sequence. An earlier study by this group[33] has shown that intermolecular triplex formation in the purine motif did not show a separate melting transition for the triplex melting. It was found that for the 13-mer sequence d-(GGGGAGGGGGAGG), the Tm of the three strand complex exceeds 5 °C the double-stranded target DNA (74 and 69 °C for the Tm of triplex and duplex, respectively). Thus, the addition of third strand stabilizes the target duplex and all the three strands (involved in duplex and triplex formation) dissociate at the same time at a temperature higher than the melting temperature of the duplex.

The melting temperature of the reported short purine motif triplex is unusually high as compared to other known triplexes. The "unusual" high stability might be due to the intramolecular (unimolecular) nature of the I-Pu DNA structure. To confirm the same and to obtain information on the molecularity of the structure formed by I-Pu, dependence of oligomer concentration on the Tm has also been investigated. It is important to mention here that while the routine spectroscopic measurements (concentration determination, normal Tm's and CD experiments) were carried out using a quartz cuvette of 1.0 cm path length, a quartz micro cuvette of 0.1 cm path length was used for the oligomer concentration dependent UV-melting experiments (Tm's). Figure 2 displays the melting profiles of I-Pu at the oligomer concentration range of 0.5−35.0 μM in 20 mM sodium cacodylate buffer (pH 7.0) containing 0.1 mM EDTA in the presence of 100 mM Na^+ (A) and 100 mM Na^+ + 10 mM Mg^{2+} (B). The Tm of the sequence at all the oligomer concentrations used was found to be constant at 81 and 96 °C in Na^+ and Na^+ + Mg^{2+} solutions, respectively. This observation is consistent with the known fact that the Tm of intramolecular (unimolecular) structures is independent of oligomer concentration.[39] Thus, this thermal melting experiment confirms the unimolecular nature of I-Pu.

The effect of Mg^{2+} on the structure and stability of d-($G_4T_4G_4$-[T]$_4$-$G_4A_4G_4$-[T]$_4$-[$C_4T_4C_4$] has also been studied by others.[40] It explained that in the absence of Mg^{2+}, the oligonucleotide adopts a hairpin duplex structure with the

dx.doi.org/10.1021/bi1012589 |*Biochemistry* 2011, 50, 4132–4142

dangling tail 5′-($G_4T_4G_4$-$[T]_4$), while in the presence of Mg^{2+}, this folds back on itself twice to give a triple helix via a double hairpin formation, with $[T]_4$ single-strand loops. Our results are in agreement with the report in which an intramolecular triplex is shown to melt in a monophasic manner. An interesting feature of purine motif TFOs is the formation of Mg^{2+} mediated high stability triplexes. As indicated by the combinatorial approach of Hardenbol and van Dyke, 13-base TFO is enough to form a stable triplex at 37 °C.[41] Moreover, purine motif TFOs sometimes show unpredictable binding affinity, which can vary from undetectable for some sequences (e.g., 5′-AGGAGGAGGAGA-3′ was not shown to form triplex in the presence of Mg^{2+})[42] to those that increase the stability of the targeted duplexes, as shown in this work.

Additionally as a control, we have also used the intermolecular version of the same sequences used for studying intramolecular triplex. Because of the symmetric nature of the target duplex, the purine strand of the target duplex, if added in excess, can act as a TFO to bind in an antiparallel fashion to the target purine strand. The purine-motif triplex forming ability of these sequences was investigated independently in $Na^+ + Mg^{2+}$. Figure 3 displays the thermal denaturation profiles of $G_2AG_5AG_2$ + $C_2TC_5TC_2$ [11Pu/11Py] at a 1:1 and 2:1 stoichiometric ratio. The denaturation profile of the combination of 11Pu + 11Py at 1:1 resulting in monophasic transition corresponds to the melting of the 11Pu•11Py duplex with a Tm of 56 °C. Changing the stoichiometric ratio of the Pu/Py oligomers to 2:1 in the same experimental solution conditions, the denaturation profile again resulted in a single transition with a Tm value of 61 °C. Usually, the melting transition of a triplex is expected to be a biphasic curve, depicting the disordering of the triplex and the duplex at varied temperatures. Occurrence of a single transition with higher Tm than the duplex could be of a stable triplex structure formed in the given 2:1 stoichiometric strand ratio. The observation is in perfect accordance with previous reports on unusually stable purine-motif triplexes.[32,33] The stability of the double-stranded target was shown to increase by binding of the purine third strand (the Tm of the triplex was greater than the duplex, manifested in single UV-melting transition showing higher Tm than the duplex melting). The melting temperatures of the triplexes were found to be the same as for the targeted duplex in the case of the 11- and 14-mer third strands, while for the 17- and 20-mer third strands, the melting temperatures of the triplexes were correspondingly 4 and 8 °C higher than for the 20-mer duplex.[32]

Interestingly, in our studies also, all three strands of the triplex were shown to open at the same time in the single melting. Binding of the 11Pu as third strand to the duplex 11Pu·11Py enhanced the Tm of the duplex by 5 °C. We observed a clear difference in the Tm's of the intermolecular triplex ($G_2AG_5AG_2$ + $C_2TC_5TC_2$) [i.e., stoichiometric ratio 2:1] and the designed intramolecular (I-Pu). The intermolecular triplex shows a Tm of 61 °C, whereas its intramolecular version melts at 96 °C. The Tm of I-Pu in the presence of Mg^{2+} seems unusually high as compared to other known triplexes. The "unusual" high stability of I-Pu is due to the intramolecular (unimolecular) nature of the I-Pu DNA structure. The differential melting under the identical solution conditions can be explained in terms of the entropy penalty of intermolecular oligonucleotide complex formation and is consistent with the conventional insight that the intermolecular triplex should form at lower temperature because of its higher unfavorable entropic contribution. This perception has already been accepted and well documented.[43]

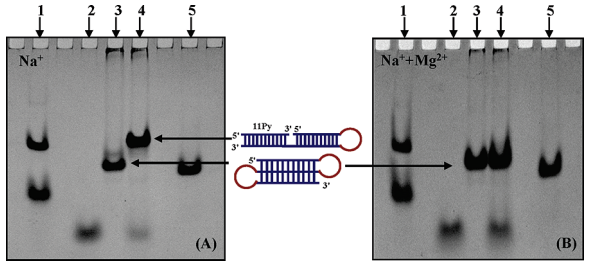

Figure 4. 20% native PAGE electrophoretic mobility pattern of the oligonucleotide sequences in 20 mM sodium cacodylate buffer (pH 7.0) and 0.1 mM EDTA containing 100 mM Na^+ (A) and 100 mM Na^+ + 10 mM Mg^{2+} (B) lane 1: PAL12, (d-CTTGAGCTCAAG), 12-mer duplex marker + PAL24, (d-CTTGAGCTTGAGCTCAAGCTCAAG), 24-mer duplex marker; lane 2: 11Py, (d-CCTCCCCCTCC); lane 3: I-Pu, (d-CCTCCCCCTCCT$_5$GGAGGGGGAGGT$_5$CCTCCCCCT-CC); lane 4: I-Pu + 11Py; lane 5: M35, (d-GACTGACTTAAG-CCGATAGCTAGCTCGATAGCTGA), 35-mer single strand.

Following section presents a correlation between the results of UV-thermal denaturation profiles and gel electrophoresis. It further establishes the formation of an intramolecular triplex, even in the absence of Mg^{2+}.

Non-Denaturating Gel Electrophoresis. Differential mobility of a sequence indicates its ability to form more than one structure, under the influence of countercations.

(a). Oligonucleotide Structure in the Presence of Sodium Ions. Non-denaturating gel electrophoresis is a very useful technique in inferring the molecularity and structure adopted by oligonucleotides. It has been extensively used to monitor and differentiate various multistranded structures. For information on various structures adopted by studied sequence I-Pu, gel electrophoresis was performed under non-denaturating conditions. Figure 4A depicts the gel electrophoretic mobility pattern of I-Pu incubated in 20 mM sodium cacodylate buffer (pH 7.0) containing 100 mM Na^+ and 0.1 mM EDTA. To predict the molecularity of the structure formed by the oligonucleotide, three size markers (PAL12, M35, and PAL24) were used as controls. PAL12 (Figure 4A, lower band in lane 1) and PAL24 (Figure 4A, upper band in lane 1) are 12-bp and 24-bp palindromic duplexes, respectively. A 35-mer single strand size marker, M35 (Figure 4A, lane 5) was also used. The 11-mer pyrimidine sequence, 11Py (d-$C_2TC_5TC_2$) (Figure 4A, lane 2), exhibited a single band and migrated faster than PAL12 (lane 1, lower band), reflecting its unstructured single-stranded status. A single band was observed for the 43-mer DNA sequence I-Pu [$C_2TC_5TC_2T_5G_2AG_5AG_2T_5G_2AG_5AG_2$] (lane 3), showing migration almost equivalent to the random 35-mer (M35) size marker (lane 5). Electrophoretic mobility of single-stranded DNA becomes almost the same as that of half length double-stranded DNA when it makes a hairpin structure,[44] and hairpins migrate faster than their corresponding unstructured single strands.[45] Thus, the migration of the 43-mer I-Pu equivalent to 35-mer random unstructured oligonucleotide clearly indicates the folded state of I-Pu, which is expected to be comprising of double hairpins, folding back twice on themselves generating an intramolecular triplex, with 11 base triplets and two $(T)_5$ loops on each side (see the cartoons between Figure 4A,B).

It is noteworthy that addition of the 11Py to I-Pu sequence resulted in an electrophoretic pattern showing two bands (Figure 4A, lane 4). The upper retarded intense band moved

Scheme 1. Scheme Illustrating the Formation of Intramolecular Triplex (I-Pu) and Intermolecular Duplex/Hairpin (I-Pu + 11Py)

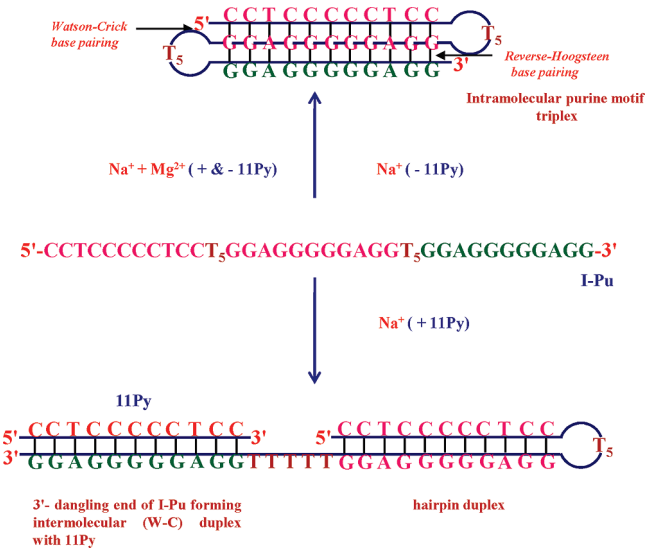

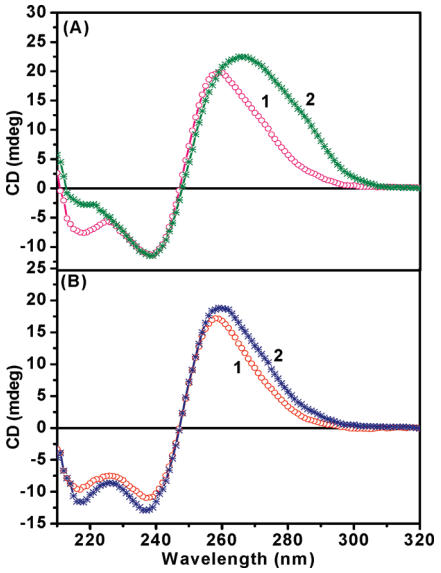

Figure 5. CD spectra of I-Pu (d-CCTCCCCCTCCT$_5$GGAGGGGGAGGT$_5$CCTCCCCCTCC) (1) and I-Pu + 11Py (d-CCTCCCCCTCC) (2) in 20 mM sodium cacodylate buffer (pH 7.0) and 0.1 mM EDTA containing 100 mM Na^+ (A) and 100 mM Na^+ + 10 mM Mg^{2+} (B).

equivalent to the used 24-bp duplex size marker (PAL24) (lane 1, upper band), whereas the fast moving lighter band (lane 4) migrated equal to the free 11Py sequence (Figure 4A, lane 2). We see that the upper band of the sample (I-Pu + 11Py) in lane 4 moved more slowly than the I-Pu band (lane 3) alone (interpreted above as intramolecular triplex). This indicates that the intramolecular triplex formation has not taken place in the presence of 11Py. Evidently, the retarded band moving equivalent to PAL24 corresponds to the intermolecular structure formed due to Watson−Crick hydrogen bonding, between the 11Py and the complementary region of unpaired flanking 3′-purine stretch of hairpin duplex of I-Pu. Since this unpaired flanking 3′-purine segment of I-Pu (in the presence of 11Py) is not involved in reverse Hoogsteen hydrogen bond formation and hence can easily be involved in W−C hydrogen bonding with its complementary 11Py sequence. This observation becomes clear by noticing the difference in band intensity of 11Py, in lane 2 and lane 4, as the observed decrease in band intensity of 11Py (in I-Pu + 11Py, lane 4) reflects the association between the two oligonucleotides (I-Pu and 11Py). The oligonucleotide concentration of 11Py used in lanes 2 and 4 was identical. The milder, lower band (lane 4) reflects the unused 11Py sequence, moving equivalent to the 11Py sequence alone (lane 2).

The possible structures adopted by I-Pu sequence in the absence or presence of 11Py sequence are modeled in Scheme 1. They include intramolecular triplex (upper) and intermolecular hairpin duplex with Watson−Crick hydrogen bonding of dangling purine stretch of I-Pu with 11Py.

(b). Oligonucleotide Structure in the Presence of Sodium and Magnesium Ions. Figure 4B represents the 20% PAGE electrophoretic mobility patterns of the studied oligonucleotides. Lane 1 shows two bands, representing 12 and 24- base pair size markers PAL12 (lower band) and PAL24 (upper band), respectively. Lane 5 showed 35-mer single-stranded size marker (M35). Lane 3 corresponds to the 43-mer I-Pu sequence in 20 mM sodium cacodylate (pH 7.0) containing 100 mM Na^+ and 10 mM Mg^{2+}. A single band with mobility higher than M35 is observed for I-Pu (lane 3), which corresponds to the intramolecular triplex.

On addition of the pyrimidine strand, 11Py, in the I-Pu sequence in the presence of sodium and magnesium ions, two distinct bands were observed (Figure 4B, lane 4). The mobility and intensity of the upper band corresponds to I-Pu sequence alone (lane 3), confirming the formation of intramolecular triplex even in the presence of 11Py, while, of the lower band (lane 4) is equivalent to the 11-Py alone (lane 2). This indicated that the 11Py has not interacted with the I-Pu sequence and remained as a free strand.

The gel experiments showed a clear correlation with thermal denaturation experiments described previously, as the I-Pu sequence on addition of 11Py in the presence of sodium showed biphasic transitions, while in the presence of sodium and magnesium, it displayed monophasic transitions (Figure 1B, curves 1 and 2, respectively), attributed to triplex melting.

An independent study by Chen[46] on similar lines, using six octadecamers with hairpin motifs, reported that sequences d-($C_4T_3G_4T_3G_4$) and d-($G_4T_3G_4T_3C_4$) form intramolecular triplexes via double hairpin formation in neutral solution and magnesium titrations indicate that magnesium is not essential for such an intramolecular triplex formation. The electrophoretic mobilities of these sequences are found to be slightly faster than that of a decameric duplex but significantly faster than that of d-($G_4T_3C_4T_3G_4$). The greater electrophoretic mobilities of d-($C_4T_3G_4T_3G_4$) and d-($G_4T_3G_4T_3C_4$) when compared to d-($G_4T_3C_4$ T_3G_4) are consistent with the expectation that they form C•G*G intramolecular triplexes, whereas d-($G_4T_3C_4T_3G_4$) oligomer forms only hairpin.

Further, we also evaluated the effect of K^+ and Ca^{2+} on the triplex forming ability of I-Pu, in the absence or presence of 11Py. Interestingly, K^+ and Ca^{2+} behaved analogously to Na^+ and Mg^{2+} toward triplex formation (data not shown).

At this point, it is important to mention that prior to running the native PAGE, the sequences were electrophoresed in gels containing 8 M urea where each of the oligomers migrated as a single band. Thus, the spectroscopic observations are substantiated

dx.doi.org/10.1021/bi1012589 |*Biochemistry* 2011, 50, 4132–4142

by gel electrophoresis for differential mobilities of inter- and intramolecular species.

Circular Dichroism Studies. The CD spectroscopy has been particularly proven to be informative in elucidating the conformations adopted by various nucleic acid secondary structures.[47] To further analyze the conformational status of structural species identified in native gel electrophoresis and UV-thermal denaturation experiments, CD measurements were performed on the I-Pu sequence. Figure 5A displays the CD spectrum of I-Pu (1) in 20 mM sodium cacodylate buffer (pH 7.0) containing 100 mM Na^+. CD spectrum of I-Pu exhibited a strong positive peak at 260 nm and a negative peak of moderate intensity centered around 240 nm. It is worth noticing that the spectrum also showed a small negative peak around 213 nm, which has previously been reported to be induced only upon triplex formation.[48−50] Such a band is characteristic of a third strand binding to the purine strand of Watson−Crick duplex through Hoogsteen hydrogen bond formation.[34,51] It can be concluded that the oligomeric structure formed by I-Pu, in the presence of sodium, is an intramolecular triplex (shown in Scheme 1). Again to reconfirm the CD signatures exhibited by intramolecular triplex, a short symmetric pyrimidine strand, 11Py, was added to the I-Pu. It is interesting to note that the characteristic feature of a triplex, that is, a negative CD peak around 213 nm in the CD spectrum (Figure 5A), has almost disappeared with the addition of 11Py in I-Pu. It appears only possible if the 3′-terminal 11Pu segment of I-Pu, which was supposed to act as a TFO instead of folding back on the central Pu segment of the I-Pu sequence, gets engaged in duplex formation with added 11Py through Watson−Crick hydrogen bonding.

Further, the addition of 11Py to I-Pu resulted in increased ellipticity of the positive signal with a 10 nm red shift to ∼270 nm (Figure 5A), which can be explained, assuming formation of a short intermolecular Watson−Crick duplex (between complementary 3′-flanking Pu region of I-Pu and added 11Py strand), along with formation of an intramolecularly folded hairpin duplex (between 5′- 11 base pyrimidine segment and central 11-base purine strand) (see the model proposed, Scheme 1). Thus, the presence of two duplexes (one inter- and other intramolecular), stabilized independently by Watson−Crick hydrogen-bonding, might be the reason for a red shift (260 → 270 nm) and simultaneous increase in CD ellipticity.

Additionally, to correlate the results of UV-thermal denaturation, gel experiments with circular dichroism, CD spectra of free I-Pu and the added pyrimidine rich symmetric stretch 11Py were also recorded in solution containing Na^+ and Mg^{2+} (Figure 5B). CD spectrum of free I-Pu shows a positive peak at 260 nm followed by negative peaks centered around 213 and 240 nm. This observation again underlines the formation of triplex by I-Pu in the presence of Na^+ and Mg^{2+}. Surprisingly, unlike the CD spectrum of Figure 5A, the addition of 11Py had very little effect on CD features, confirming the presence of integral triplex even in the presence of Py strand, showing complementarity to the 3′- I-Pu segment.

Interpretation of CD relies largely on the pragmatic associations of spectra with known polymer conformations. Guanine-rich molecules of DNA invariably provide A-like CD spectra to which intrastrand guanine−guanine stacking is the dominant contribution.[52] Previous study on similar lines, demonstrating CD spectrum of G-rich 20-mer oligopurine•oligopyrimidine target with 75% GC content, showed an A-type DNA CD signatures, in the presence of 10 mM Mg^{2+} and 50 mM Na^+ in 20 mM-Tris HCl (pH 7.5).[32] Upon triplex formation with purine TFO, the A-DNA form was reported to be more prominent. This observation is in accordance with our present study, where the 260 nm positive peak along with 240 and 213 nm negative CD signals, identified for I-Pu triplex can be interpreted as A-type DNA. An interesting observation in this experiment was that, in the presence of 11Py, the intramolecular triplex (in sodium) is disrupted with notable change in CD spectrum corresponding to an increase in positive amplitude followed by 10 nm red shift (Figure 5A), whereas the intramolecular triplex (in sodium and magnesium) remains intact with hardly any affect on CD spectrum (Figure 5B). It is fairly possible that inter- and intramolecular (hairpin) duplexes (formed as a result of 11Py addition to I-Pu) have some B-type DNA content accountable for the 270 nm positive peak.[53,54] This triplex → duplex equilibrium is limited to sodium-mediated intramolecular I-Pu triplex formation, as no such transition was observed in magnesium-mediated intramolecular triplex formation. Our observation here also made it conceivable that in order to accommodate a third strand in triplex formation, the backbone of the B-DNA duplex has to be adjusted into A-like DNA.[32,55]

We hypothesize that the presence of divalent magnesium ions makes the reverse-Hoogsteen hydrogen bonding of intramolecular triplex so stable that even in the presence of complementary pyrimidine strand, it does not welcome Watson−Crick hydrogen bonding to form intermolecular duplex. This further confirms that the I-Pu strand exists as an intramolecular triplex irrespective of the presence or absence of Mg^{2+} ions; nevertheless, Mg^{2+} stabilized the same, possibly due to the formation of a continuous spine on G N7.[29] Similarly, a recent study states that in the case of G-rich oligonucleotides, triplex formation is principally dependent on the percent of G and length of TFO.[56]

Because of the phosphate backbone, DNA is highly negatively charged and metal cations play a crucial role in stabilizing multistranded DNA structures. Although the cationic effects on the formation and stability of triplexes have been studied in detail, the transition characteristic and thermodynamic properties of the triplex formation, especially the effect of Hoogsteen strand on the local and global triplex in response to various divalent cations are still not fully understood. A large number of research groups have examined this aspect and described the effect of the presence and position of bases, various cations on the basis of charge-to-ionic radius ratio, and thermodynamic reasons for the stability of inter- and intramolecular triplexes.

Along a triplex, the negatively charged phosphate per nucleotide creates a high linear charge density. As a requirement, countercations have to be involved to reduce the phosphate−phosphate repulsion, especially around the grooves. Cations can either screen the negative charges globally or associate with phosphate groups physically.[57] Type I (Py-motif) T/U(A•T/U) triplexes only require monovalent Na^+, while Type II (Pu-motif) G(G•C) triplexes, however, are not as often observed without divalent (Mg^{2+}) ions. This specific ionic effect appears to depend on the structural difference between these triplexes, and a clear conformation−counterion relationship for the triplex stabilization can be obtained from this observation. Type I triplexes require only counterions with a low charge-to-ionic radius ratio (e.g., Na^+), but type II triplexes need a higher ratio (e.g., Mg^{2+}, Ca^{2+}). For heterogeneous triplexes with dinucleotide repeat sequences, even smaller cations such as Zn^{2+} are necessary. Differences in the hydration shell structure accompanying various counterions may be the determining factor. Wan et al. in

2009 using electrospray ionization mass spectrometry (ESI-MS) reported that the stabilization of divalent cations to purine-rich triplexes is in the order of $Co^{2+} \approx Ni^{2+} > Zn^{2+} > Cu^{2+} \approx Mn^{2+} > Mg^{2+} > Ca^{2+}$.[58] Besides binding phosphate, divalent cations have been found to interact with various sites on nucleic acid, including N7 and O7 of guanine.[59,60] When an electrophile interacts with N7, the formation of reverse-Hoogsteen hydrogen bonds would be enhanced since NH2 and N1H protons of guanine in the third strand should become more acidic, thus improving the stability of the purine-rich triplex.[61−64]

Some of us have previously[65] suggested that the selected sequences for pu-motif triplex formation should have a high G content and especially the G residues should lie in stretches. The Mg^{2+} cations are statistically close to the G N7 and relatively far from the A N7. The presence of an A repels the Mg^{2+} from adjacent G residues. Therefore, the triplexes are stabilized when the Mg^{2+} can form a continuous spine on G N7. Mg^{2+} cations bind to guanines more strongly than does Na^+. The triplex with the higher guanine content has a lower energy. From the comparison of the two triplexes with the same guanine content, it may be concluded that Mg^{2+} ions have a higher binding affinity to guanine stretches. It was reported that the negative potential of the N7 lone pair is even deeper because of the nearby presence of the O6 atom on the same residue. On an adenine, the positive potential created by the amino group acts in the other direction, preventing aggregation of Mg^{2+} and destabilizing the triplex. In a stretch of G residues, the negative potential is decreased by the proximity of the N7 and O6 atoms of the adjacent G residues and this favors the binding of Mg^{2+}. Therefore, the stability does not depend only on the global G content of the TFO but also on the sequence.

To explain the effect of cations on nucleic acids stability, there have been two successful polyelectrolyte theories: the counterion condensation (CC) theory and the Poisson−Boltzmann (PB) theory. Recently, to treat the correlations and fluctuations for bound ions, a tightly bound ion (TBI) theory was also developed. It was shown that the 1 M NaCl solution has effectively the equivalent ionic effect on the helix stability as the 10 mM $MgCl_2$/150 mM NaCl mixed solution. TBI theory explained the dependence of stability on helix length from the enthalpy−entropy competition in the ion-binding process.[66] The ion-binding entropic penalty for $[Mg^{2+}]$ = 10 mM is much larger than that for $[Na^+]$ = 1 M. Therefore, entropically, Mg^{2+} binding is less favorable than Na^+ binding. However, enthalpically, the binding of Mg^{2+}, which carries a higher charge and can cause more efficient charge neutralization, is more favorable than that of Na^+. Therefore, the enthalpic effect becomes more important for a longer helix, which has stronger electric field near the DNA surface. As a result, as the helix length is increased, Mg^{2+} would stabilize the helix more effectively than Na^+.

Theoretical studies by Jordi et al. in 2002 showed the large stabilizing effect of the Mg^{2+} cation on the C•G*G triplet which mainly arises from the balance of electrostatic interactions between the cation with the three bases in the triplet.[67] However, the cation-induced polarization, which is largely concentrated in the Hoogsteen guanine, also makes a significant contribution to the stabilization of the triplet. The interaction energy of the triplet with and without the pentahydrated Mg^{2+} cation was calculated, which was around 100 kcal/mol larger in the presence of the Mg^{2+} cation, which mainly stems from the interaction of the cation with the Hoogsteen-like guanine (−87.1 kcal). There is also a favorable interaction of the cation with the Watson−Crick guanine (−14.2 kcal/mol), which can be explained by the favorable electrostatic interaction of the cation with the negative electrostatic potential generated by N7 and O6 atoms of the Watson−Crick guanine. In contrast, the interaction of the cation with cytosine is disfavored by +9.7 kcal/mol, as expected from the positive electrostatic potential created by the amino group of cytosine. The difference between the total energy and the sum of pairwise interaction energies must be attributed to the threebody term, which is around −8 kcal/mol more favorable in the N7-bound cation complex than in the isolated triplet. Overall, the energies of the N7-bound cation Hoogsteen and reverse−Hoogsteen G-G pairs differ by less than 2 kcal/mol. Therefore, it can be stated that the cation-induced stabilization of the C•G*G triplet must be (i) comparable in both Hoogsteen and reverse−Hoogsteen arrangements and (ii) sensibly larger than for the A-A.T trio, because the interaction energy of the hydrated $Mg^{2+}\cdots$G-G complex is around 70 kcal/mol larger than for the hydrated $Mg^{2+}\cdots$A-A complex.

The intriguing behavior of monovalent Na^+ conferring stabilization to intramolecular purine-motif triplex and partially compensating the requirement of Mg^{2+} cation could be only due to the compact and rigid conformation of the intramolecular triplex. The strengthening of the reverse−Hoogsteen type hydrogen bonds due to the compact nature of structure, the affinity of monovalent Na^+ toward charge neutralization seems to be sufficient to exert considerable formation of the triplex. Once formed in the presence of Na^+, the I-Pu stabilized by Mg^{2+} behaved like normal intermolecular Pu-motif triplexes.

BIOLOGICAL SIGNIFICANCE

Investigators have suggested that secondary structures in DNA may be involved with physiologic gene regulatory processes in higher organisms. In view of the superfluity of literature and our perspective, this hypothesis has not been difficult to prove. The understanding of the structural features of triplexes is essential for the study of their biological functions and applications. Do natural DNA triple-helical structures occur and function in vivo ? This vital question has been intriguing scientists working in this area worldwide. A number of excellent reviews on the potential use of DNA triple-helical structures in oligonucleotide therapeutics and biotechnological applications have appeared in recent times.[23,68−72] However, direct and unambiguous evidence of possible biological roles of these structures is yet hard to pin down. The extensive literature conveys that there seems a justified optimism for the eventual feasibility and therapeutic benefits of gene targeting strategies.

Intramolecular triplex could be formed within a single homopurine−homopyrimidine duplex DNA region in supercoiled DNA, which generated interest in these studies because many sequences in the human genome have a potential to form intramolecular triplex structures. Uses of bioinformatics and pattern recognition programs have been made to search genetic databases for sequences with the potential to form intrastrand triple helices.[73] Several prokaryotic genomes yielded provocative families of sequence elements with this potential.

Intramolecular triplex DNA might influence the regulation of gene expression in a number of different ways. The association of a third strand with a duplex is a thermodynamically weaker and kinetically slower process than duplex formation.[74] Hence, various approaches have been undertaken in order to enhance the binding of the third strand under physiological conditions

which includes use of monovalent or divalent cations, attaching intercalators to the third strand oligonucleotides, photoactivated cross-linking agents, use of triplex selective ligands, and interaction of peptide/protein with DNA triplex. The enhanced stability relative to pyr•pur*pyr triplexes, coupled with the lack of a requirement for acidic pH, make pyr•pur*pur triplexes appealing choices for use as sequence-specific artificial nucleases and regulators of gene expression in vitro and in vivo. Several proteins have been recognized to interact specifically with purine-motif triplex structures.[75,76] A high degree of structural polymorphism shown by homopurine•homopyrimidine sequences, resulted in the formation of pyr•pur*pur triplex. This intramolecular triplex (H-DNA) formation is facilitated by negative supercoiling and mere presence of zinc ions.[77] The data accumulated on intramolecular DNA triplexes strongly suggest that they may exist in vivo and may be involved in a number of DNA information flow processes in a family of genes that accommodate the appropriate oligopyrimidine•oligopurine mirror repeat sequences in their regulatory regions.[68] Demonstration of the ability of TFOs to deliver mutagenic agents to DNA in a site-specific manner, and the role of TFOs in inducing gene modification in chromosomal DNA via the effect of triple helix itself, lay the foundation of the potential application of these molecules in human gene therapy.[78]

It is true that the studied 11-bp duplex Pu•Py target sequence is common to some of the cellular genes along with disease causing genes; however, for targeting the disease-related targets for therapeutic purpose through triplex strategy, the specificity will come from the longer targets which include the flanking sequences of 11-bp duplex. For example, human *c-jun* protooncogene carries a highly conserved 21-bp long polypurine•polypyrimidine at the 3′-region, 20-bp in the *vpx* gene of *SIV* and *HIV-2*, 13-bp at promoter region of murine *c-pim*-1 protooncogene.

It is important to mention that although intramolecular triplexes lack obvious therapeutic applications, they have the potential to arise in natural systems. It is well established that homopurine and homopyrimidine stretches are abundant in eukaryotic genomes including mammalian genomes and are frequently located near regulatory regions and in recombination hotspots.[79] Such sequence with mirror repeat can adopt an intramolecular triplex. Such structures could occur during local denaturation of duplex DNA containing such repeats allowing one strand to fold back forming base triplets with the adjacent native duplex DNA.

Intramolecular triplexes play important roles in vivo and are inherently mutagenic and recombinogenic, such that elements of triplex structures may be pharmacologically exploitable.[72] The evidence for DNA repair of triplex-associated lesions by nucleotide excision repair pathway are examined in a recent review.[80]

Since in this study the I-Pu is designed to model an intramolecular triplex, though containing the natural 11-bp homopyrimidine•homopurine sequence, our conclusions are perhaps not directly relevant to cellular regulation. However, the data reported here, might be important in providing insights into the role of sequences and cations on triplex formation. An obvious limitation to the natural occurrence of intrastrand DNA triple helices is the requirement that all three domains be available along a single-strand DNA. However, the unusual stability discovered here due to the sequence-dependent conformation factor can tolerate a substantial amount of sequence imperfections for intramolecular triplex formation. It will therefore be of interest to explore genomes for sequences with the potential to adopt or encode intrastrand triple helices, as the discovery of similar sequences in genomes could indicate potential structural and functional roles in vivo.

CONCLUSION

To sum up, based on native gel electrophoresis, UV-thermal denaturation, and circular dichroism spectroscopic studies, we conclude that the formation of intramolecular purine motif triplex containing a symmetrical Pu•Py segment (G_2AG_5-AG_2)•($C_2TC_5TC_2$) of human *c-jun* protooncogene takes place in the presence of sodium; however, the presence of magnesium provides further stabilization to the same. Thermal denaturation studies reveal that the helix-to-coil transitions of the I-Pu strand alone are monophasic in the absence as well as in the presence of magnesium, reflecting the dissociation of triplex to single strand in one step. Further, the addition of an 11-mer symmetrical sequence, 5′-CCTCCCCCTCC-3′ (11Py) to I-Pu, resulted in a biphasic melting profile, in sodium ions. The lower temperature melting transition corresponds to the disordering of an intermolecular (Watson−Crick) duplex formed between added 11Py and 3′- purine stretch of I-Pu, whereas the higher temperature transition matches the melting of 11-base pairs intramolecular hairpin with a $(T)_5$ loop (model proposed, Scheme 1). However, the addition of 11Py to I-Pu in the presence of magnesium resulted in a monophasic transition revealing a single step melting of intramolecular triplex (I-Pu).

The results of UV-melting studies were confirmed by native gel assays in buffer containing magnesium as well as sodium ions. The single bands with identical migration were obtained in magnesium gel, for each of I-Pu and I-Pu + 11Py, whereas the migration of the said bands varied in sodium alone. It is demonstrated that I-Pu forms an intramolecular triplex structure in the absence as well as in the presence of magnesium. Results of gel studies correlate well with CD observations. CD spectrum of I-Pu displayed classical A-type DNA features and signatures of triplex in sodium as well as in magnesium solutions. The sodium triplex destabilizes in the presence of an added complementary 11Py oligonucleotide, due to formation of a Watson−Crick duplex at the 3′-terminal segment of I-Pu and 11Py. On the other hand, the magnesium triplex of I-Pu remain unaltered in the said situation, highlighting its stable status.

This study concludes that the presence of Mg^{2+} ions is not obligatory for the formation of intramolecular purine motif triplex. Nonetheless, its presence adds to the stability of the triple-stranded structures. The literature reveals that purine-motif triplex formation in the "intermolecular" mode requires divalent cation, that is, magnesium, while their intramolecular versions can survive with monovalent cation sodium. Further, it can be said that the reverse−Hoogsteen hydrogen bonds formed in the presence of magnesium ions are more stable than formed in the presence of sodium ions, making them favored over Watson−Crick base pairing. On the contrary, when intramolecular triplex formation is facilitated by monovalent Na^+, it is the Watson−Crick bonding that prevails over reverse−Hoogsteen base pairing. As a consequence, we found the I-Pu sequence an interesting example of intramolecular triple helix, and the data reported here might be important in providing insights into the role of cations on triplex formation.

AUTHOR INFORMATION

Corresponding Author

*Tel: +91-11-27666726. Fax: +91-11-27667794. E-mail: skukreti@chemistry.du.ac.in; kukretishrikant@yahoo.com.

Funding Sources

This work was supported by Research Grant No. SP/SO/D-21/2001 funded by Department of Science and Technology (DST), Govt of India.

REFERENCES

(1) Felsenfeld, G., Davies, D. R., and Rich, A. (1957) Formation of a three-stranded polynucleotide molecule. *J. Am. Chem. Soc. 79*, 2023–2024.

(2) Thuong, N. T., and Helene, C (1993) Sequence-specific recognition and modification of double-helical DNA. *Angew. Chem., Int. Ed. Engl. 32*, 666–690.

(3) Mirkin, S. M., and Frank-Kamenetskii, M. D. (1994) H-DNA and related structures. *Annu. Rev. Biophys. Biomol. Struct. 23*, 541–576.

(4) Sun, J. S., and Helene, C. (1993) Oligonucleotide-directed triple-helix formation. *Curr. Opin. Struct. Biol. 3*, 345–356.

(5) Husler, P. L., and Klump, H. H. (1995) Prediction of pH dependent properties of DNA triple helices. *Arch. Biochem. Biophys. 317*, 46–56.

(6) Lavelle, L., and Fresco, J. R. (1995) UV spectroscopic identification and thermodynamic analysis of protonated third strand deoxycytidine residues at neutrality in the triplex $d(C(^{+})\text{-}T)_6$: $[d(A\text{-}G)_6 \bullet d(C\text{-}T)_6]$: Evidence for a proton switch. *Nucleic Acids Res. 23*, 2692–2705.

(7) Asensio, J. L., Lane, A. N., Dhesi, J., Bergqvist, S., and Brown, T. (1998) The contribution of cytosine protonation to the stability of parallel DNA triple helices. *J. Mol. Biol. 275*, 811–822.

(8) Lee, J. S., Woodsworth, M. L., Latimer, L. J., and Morgan, A. R. (1984) Poly(pyrimidine).poly(purine) synthetic DNAs containing 5-methyl cytosines form stable triplexes at neutral pH. *Nucleic Acids Res. 12*, 6603–6614.

(9) Frank-Kamenetskii, M. D., and Mirkin, S. M. (1995) Triplex DNA structures. *Annu. Rev. Biochem. 64*, 65–95.

(10) Francois, J. S., Lacoste, J., Lacroix, J., and Mergny, J. L. (2000) Design of antisense and triplex forming oligonucleotides. *Methods Enzymol. 313*, 74–95.

(11) Sun, J. S., De-Bizemont, T., Duval-Valentin, G., Montenay-Garestier, T., and Helene, C. (1991) Extension of the range of recognition sequences for triple helix formation by oligonucleotides containing guanines and thymines. *C. R. Acad. Sci. III 313*, 585–590.

(12) Durland, R. H., Kessler, D. J., Gunnell, S., Duvic, M., Pettitt, B. M., and Hogan, M. E. (1991) Binding of triple helix forming oligonucleotides to sites in gene promoters. *Biochemistry 30*, 9246–9255.

(13) Buchini, S., and Leumann, C. J. (2003) Recent improvements in antigene technology. *Curr. Opin. Chem. Biol. 7*, 717–726.

(14) Mirkin, S. M., Lyamichev, V. I., Drushlyak, K. N., Dobrynin, V. N., Filippov, S. A., and Frank-Kamenetskii, M. D. (1987) DNA H-form requires a homopurine-homopyrimidine mirror repeat. *Nature 330*, 495–497.

(15) Kohwi, Y., and Kohwi-Shigematsu, T. (1988) Magnesium ion-dependent triple-helix structure formed by homopurine-homopyrimidine sequences in supercoiled plasmid DNA. *Proc. Natl. Acad. Sci. U.S.A. 85*, 3781–3785.

(16) Shimizu, M., Hanvey, J. C., and Wells, R. D. (1989) Intramolecular DNA triplexes in supercoiled plasmids. Effect of loop size on formation and stability. *J. Biol. Chem. 264*, 5944–5949.

(17) Htun, H., and Dahlberg, J. E. (1989) Topology and formation of triple-stranded H-DNA. *Science 243*, 1571–1576.

(18) Ussery, D. W., and Sinden, R. R. (1993) Environmental influences on the in vivo level of intramolecular triplex DNA in *Escherichia coli*. *Biochemistry 32*, 6206–6213.

(19) Chan, P. P., and Glazer, P. M. (1997) Triplex DNA: fundamentals, advance and potential applications for gene therapy. *J. Mol. Med. 75*, 267–282.

(20) Giovannangeli, C., and Helene, C. (1997) Progress in developments of triplex -based strategies. *Antisense Nucleic Acid Drug Dev. 7*, 413–421.

(21) Casey, B. P., and Glazer, P. M. (2001) Gene targeting via triple helix formation. *Prog. Nucleic Acid Res. Mol. Biol. 67*, 163–192.

(22) Faria, M., and Ulrich, H. (2002) The use of synthetic oligonucleotides as protein inhibitors and anticode drugs in cancer therapy: accomplishments and limitations. *Curr. Cancer Drug Targets 2*, 355–368.

(23) Simon, P., Cannata, F., Concordet, J. P., and Giovannangeli, C. (2008) Targeting DNA with triplex-forming oligonucleotides to modify gene sequence. *Biochimie 90*, 1109–1116.

(24) Maher, L. J., III, Wold, B., and Dervan, P. B. (1989) Inhibition of DNA binding proteins by oligonucleotide-directed triple helix formation. *Science 245*, 725–730.

(25) Hanvey, J. C., Shimizu, M., and Wells, R. D. (1990) Site-specific inhibition of EcoRI restriction/modification enzymes by a DNA triple helix. *Nucleic Acids Res. 18*, 157–161.

(26) Strobel, S. A., Doucette-Stamm, L. A., Riba, L., Housman, D. E., and Dervan, P. B. (1991) Site-specific cleavage of human chromosome 4 mediated by triple-helix formation. *Science 254*, 16939–16942.

(27) Faucon, B., Mergny, J. L., and Helene, C. (1996) Effects of third strand composition on the triple helix formation: Purine versus pyrimidine oligonucleotides. *Nucleic Acids Res. 24*, 3181–3188.

(28) Mills, M., Arimondo, P. B., Lacroix, L., Garestier, T., Klump, H., and Mergny, J. L. (2002) Chemical modification of the third strand: differential effects on purine and pyrimidine triple helix formation. *Biochemistry 41*, 357–366.

(29) Debin, A., Laboulais, C., Ouali, M., Malvy., C., Le Bret, M., and Svinarchuk, F. (1999) Stability of G, A triple helices. *Nucleic Acids Res. 27*, 2699–2707.

(30) Bader, B. L, Magin, T. M., Hatzfeld, M., and Franke, W. W. (1986) Amino acid sequence and gene organization of cytokeratin no. 19, an exceptional tail-less intermediate filament protein. *EMBO J. 5*, 1865–1875.

(31) Wu, L. C., Morley, B, J., and Campbell, R. D. (1987) Cell-specific expression of the human complement protein factor B gene: evidence for the role of two distinct 5′-flanking elements. *Cell 48*, 331–342.

(32) Svinarchuk, F., Monnot, M., Merle, A., Malvy, C., and Fermandjian, S. (1995) The high stability of the triple helices formed between short purine oligonucleotides and SIV/HIV-2 vpx genes is determined by the targeted DNA structure. *Nucleic Acids Res. 23*, 3831 3836.

(33) Svinarchuk, F., Paoletti, J., and Malvy, C. (1995) An unsually stable purine (purine-pyrimidine) short triplex. *J. Biol. Chem. 270*, 14068–14071.

(34) Plum, G. E., and Breslauer, K. J. (1995) Thermodynamics of an intramolecular DNA triple helix: a calorimetric and spectroscopic study of the pH and salt dependence of thermally induced structural transitions. *J. Mol. Biol. 248*, 679–695.

(35) Sklenar, V., and Feigon, J. (1990) Formation of a stable triplex from a single DNA strand. *Nature 345*, 836–838.

(36) Radhakrishanan, I., Santor, C. D. L., and Patel, D. J. (1991) NMR structural studies of intramolecular purine•purine•pyrimidine DNA triplexes in solution: Base pairing alignments and strand direction. *J. Mol. Biol. 221*, 1403–1418.

(37) Puglisi, J. D., and Tinoco, I., Jr. (1989) Absorbance melting curves of RNA. *Methods Enzymol. 180*, 304–325.

(38) Pilch, D. S., Levenson, C., and Shafer, R., H. (1991) Structure, stability and thermodynamics of a short Intermolecular Purine-Purine-Pyrimidine triple helix. *Biochemistry 30*, 6081–6087.

(39) Marky, L. A., Blumenfeld, K. S., Kozlowski, S., and Breslauer, K. J. (1983) Salt-dependent conformational transitions in the self-complementary deoxydodecanucleotide d(CGCAATTCG CG): evidence for hairpin formation. *Biopolymers 22*, 1247–1257.

(40) Gondeau, C., Maurizot, J., C., and Durand, M. (1998) Spectroscopic investigation of an intramolecular DNA triplex containing both G.G.C and T.A.T triads and its complex with netropsin. *J. Biomol. Struct. Dyn. 15*, 1133–1145.

(41) Hardenbol, P., and Van Dyke, M. W. (1996) Sequence specificity of triplex DNA formation: Analysis by a combinatorial approach, restriction endonuclease protection selection and amplification. *Proc. Natl. Acad. Sci. U.S.A. 93*, 2811–2816.

(42) Malkov, V. A., Voloshin, O. N., Soyfer, V. N., and Frank-Kamenetskii, M. D. (1993) Cation and sequence effects on stability of intermolecular pyrimidine-purine-purine triplex. *Nucleic Acids Res. 21*, 585–591.

(43) Soto, A. M., Loo, J., and Marky, L. A. (2002) Energetic contributions for the formation of TAT/TAT, TAT/CGC(+), and CGC(+)/CGC(+) base triplet stacks. *J. Am. Chem. Soc. 124* (48), 14355–63.

(44) Xodo, E., Manzini, G., Quadrifoglio, F., Yathindra, M., van der Marcel, G. A., and Van Boom, J. H. (1989) A facile duplex-hairpin interconversion through a cruciform intermediate in a linear DNA fragment. *J. Mol. Biol. 205*, 777–781.

(45) Kejnovska, I., Tumova, M., and Vorlickova, M. (2001) CGA)-(4): parallel, anti-parallel, right-handed and left-handed homoduplexes of a trinucleotide repeat DNA. *Biochim. Biophys. Acta 1527*, 73–80.

(46) Chen, F. M. (1991) Intramolecular triplex formation of the purine•purine• pyrimidine type. *Biochemistry 30*, 4472–4479.

(47) Kypr, J., Kejnovska, I., Renciuk, D., and Vorlickova, M. (2009) Circular dichroism and conformational polymorphism of DNA. *Nucleic Acids Res. 37*, 1713–1725.

(48) Manzini, G., Xodo, L. E., Gasparotto, D., Quadrifoglio, F., van der Marel, G. A., and van Boom, J. H. (1990) Triple helix formation by oligopurine-oligopyrimidine DNA fragments. Electrophoretic and thermodynamic behavior. *J. Mol. Biol. 213*, 833–843.

(49) Xodo, L. E., Manzini, G., and Quadrifoglio, F. (1990) Spectroscopic and calorimetric investigation on the DNA triplex formed by d(CTCTTCTTTCTTTTCTTTCTTCTC) and d(GAGAAGAAAGA) at acidic pH. *Nucleic Acids Res. 18*, 3557–3564.

(50) McShan, W. M., Rossen, R. D., Laughter, A. H., Trial, J., Kessler, D. J., Zendegui, J. G., Hogan, M. E., and Orson, F. M. (1992) Inhibition of transcription of HIV-1 in infected human cells by oligodeoxynucleotides designed to form DNA triple helices. *J. Biol. Chem. 267*, 5712–5721.

(51) Liu, K., Miles, H. T., Frazier, J., and Sasisekharan, V. (1993) A novel DNA duplex. A parallel-stranded DNA helix with Hoogsteen base pairing. *Biochemistry 32*, 11802–11809.

(52) Kypr, J., and Vorlickova, M. (2002) Circular dichroism spectroscopy reveals conformation of guanine runs in DNA. *Biopolymers 67*, 275–277.

(53) Gray, D. M., Ratliff, R. L., and Vaughan, M. R. (1992) Circular dichroism spectroscopy of DNA. *Methods Enzymol. 211*, 389–406.

(54) Ivanov, V. I., and Krylov, D. Y. (1992) A-DNA in solution as studied by diverse approaches. *Methods Enzymol. 211*, 111–127.

(55) Cheng, Y. K., and Pettitt, B. M. (1995) Solvent effects on model $d(CG.G)_7$ and $d(TA.T)_7$ DNA triple helices. *Biopolymers 35*, 457–473.

(56) Vekhoff, P., Ceccaldi, A., Polverari, D., Pylouster, J., Pisano, C., and Arimondo, P. B. (2008) Triplex formation on DNA targets: how to choose the oligonucleotide. *Biochemistry 47*, 12277–12289.

(57) Cheng, Y.-K., and Pettitt, B. M. (1992) Stabilities of double- and triple-strand helical nucleic acids. *Prog. Biophys. Mol. Biol. 58*, 225–257.

(58) Wan, C., Cui, M., Song, F., Liu, Z., and Liu, S. (2009) Evaluation of effects of bivalent cations on the formation of purine-rich triple-helix DNA by ESI-FT-MS. *J. Am. Soc. Mass Spectrom. 20*, 1281–1286.

(59) Gao, Y.-G., Sriram, M., and Wang, A. H.-J. (1993) Crystallographic studies of metal ion−DNA interactions: Different binding modes of cobalt(II), copper(II) and barium(II) to N7 of guanines in Z-DNA and a drug−DNA complex. *Nucleic Acids Res. 21*, 4093–4101.

(60) Bhattacharyya, R. G., and Nayak, K. K. (1988) Interaction of $Mg{\cdot}ATP^{2+}$ with DNA: Assessment of metal binding sites and DNA conformations by spectroscopic and thermal denaturation studies. *Inorg. Chim. Acta 153*, 79–86.

(61) Floris, R., Scaggiante, B., Manzini, G., Quadrifoglio, F., and Xodo, L. E. (1999) Effect of cations on purine·purine·pyrimidine triple helix formation in mixed-valence salt solutions. *Eur. J. Biochem. 260*, 801–809.

(62) Potaman, V. N., and Soyfer, V. N. (1994) Divalent metal cations upon coordination to the N7 of purines differentially stabilize the Py.Pu.Pu DNA triplex due to unequal Hoogsteen-type hydrogen bond enhancement. *J. Biomol. Struct. Dyn. 11*, 1035–1040.

(63) Sponer, J., Sabat, M., Burba, J. V., Doody, A. M., Leszczynski, J., and Hobza, P. (1998) Stabilization of the purine.purine.pyrimidine DNA base triplets by divalent metal cations. *J. Biomol. Struct. Dynam. 16*, 139–143.

(64) Sponer, J., Sabat, M., Gorb, L., Leszczynski, J., Lippert, B., and Hobza, P. (2000) The effect of metal binding to the N7 site of purine nucleotides on their structure, energy, and involvement in base pairing. *J. Phys. Chem. B 104*, 7535–7544.

(65) Debin, A., Laboulais, C., Ouali, M., Malvy, C., Le bret, M., and Svinarchuk, F. (1999) Stability of G, A triple helices. *Nucleic Acids Res. 27* (13), 2699–2707.

(66) Tan, Z.-J., and Chen, S.-J. (2006) Nucleic acid helix stability: Effects of salt concentration, cation valence and size, and chain length. *Biophys. J. 90*, 1175–1190.

(67) Munoz, J., Gelpı, J. L., Soler-Lopez, M., Subirana, J.A., Orozco, M., and Luque, F. J. (2002) Can Divalent metal cations stabilize the triplex motif? Theoretical study of the interaction of the hydrated Mg^{2+} cation with the G-G.C triplet. *J. Phys. Chem. B. 106*, 8849–8857.

(68) Zain, R., and Sun, J. S. (2003) Do natural DNA triple-helical structures occur and function in vivo? *Cell. Mol. Life Sci. 60*, 862–870.

(69) Duca, M., Vekhoff, P., Oussedik, K., Halby, L., and Arimondo, P. B. (2008) The triple helix: 50 years later, the outcome. *Nucleic Acids Res. 36*, 5123–5138.

(70) Schleifman, E. B., Chin, J. Y., and Glazer, P. M. (2008) Triplex-mediated gene modification. *Methods Mol. Biol. 435*, 175–190.

(71) Mirkin, S. M. (2008) Discovery of alternative DNA structures: a heroic decade (1979−1989). *Front. Biosci. 13*, 1064–1071.

(72) Jain, A., Wang, G., and Vasquez, K. M. (2008) DNA triple helices: biological consequences and therapeutic potential. *Biochimie 90*, 1117–1130.

(73) Hoyne, P. R., Edwards, L. M., Viari, A., and Maher, L. J., III (2000) Searching genomes for sequences with the potential to form intrastrand triple helices. *J. Mol. Biol. 302*, 797–809.

(74) Shafer, R. H. (1998) *Progress in Nucleic Acid Research* (Moldave, K., Ed.) Vol. 59, pp 55−94, Academic Press, San Diego, CA.

(75) Musso, M., Nelson, L. D., and Van Dyke, M. W. (1998) Characterization of purine-motif triplex DNA-binding proteins in HeLa extracts. *Biochemistry 37*, 3086–3095.

(76) Nelson, L. D., Musso, M., and Van Dyke, M. W. (2000) The yeast STM1 gene encodes a purine motif triple helical DNA-binding protein. *J. Biol. Chem. 275*, 5573–5581.

(77) Bernues, J., Beltran, R., Casasnovas, J. M., and Azorín, F. (1989) Structural polymorphism of homopurine-homopyrimidine sequences: the secondary DNA structure adopted by a $d(GA.CT)_{22}$ sequence in the presence of zinc ions. *EMBO J. 8*, 2087–2094.

(78) Kalish, J. M., and Glazer, P. M. (2005) Targeted genome modification via triple helix formation. *Ann. N.Y. Acad. Sci. 1058*, 151–161.

(79) Schroth, G. P., and P. Shing Ho, P. (1995) Occurrence of potential cruciform and H-DNA forming sequences in genomic DNA. *Nucleic Acids Res. 23* (11), 1977–1983.

(80) Chin, J. Y., and Glazer, P. M. (2009) Repair of DNA lesions associated with triplex-forming oligonucleotides. *Mol. Carcinog. 48*, 389–399.